Diffusely charged polymeric zwitterions as loosely hydrated marine antifouling coatings

Shawn D. Mengel[1], Wen Guo[2], Guangyao Wu[2], John A. Finlay[3], Peter Allen[3], Anthony S. Clare[3], Riddhiman Medhi[4], Zhan Chen[2], Christopher K. Ober[4], Rachel A. Segalman[1,5,6*]

[1]Department of Chemical Engineering, University of California, Santa Barbara, California 93106 U.S.A.
[2]Department of Chemistry, University of Michigan, Ann Arbor, Michigan 48103 U.S.A.
[3]School of Natural and Environmental Sciences, Newcastle University, Newcastle upon Tyne NE1 7RU U.K.
[4]Department of Materials Science and Engineering, Cornell University, Ithaca, New York 14583 U.S.A.
[5]Department of Materials, University of California, Santa Barbara, California 93106 U.S.A.
[6]Department of Chemistry & Biochemistry, University of California, Santa Barbara, California 93106 U.S.A.

*Corresponding author. Email: segalman@ucsb.edu

Abstract

Polymeric zwitterions exhibit exceptional fouling resistance through formation of a strongly hydrated surface of immobilized water molecules. While extensively tested for their performance in biomedical, membrane, and, to a lesser extent, marine environments, few studies have investigated how the molecular design of the zwitterion may enhance this performance. Further, while theories of zwitterion antifouling mechanisms exist for molecular-scale foulant species (e.g., proteins), it remains unclear how molecular-scale mechanisms influence the micro- and macroscopic interactions of relevance to marine applications. The present study addresses these gaps through use of a modular zwitterion chemistry platform, which is characterized by a combination of surface-sensitive sum frequency generation (SFG) vibrational spectroscopy and marine assays. Zwitterions with increasingly delocalized cations demonstrate improved fouling resistance against the green alga *Ulva linza*. SFG spectra correlate well with the assay results, suggesting that the more diffuse charges exhibit greater surface hydration with more bound water

molecules. Hence, the number of bound interfacial water molecules appears to be more influential in determining marine antifouling activities of zwitterionic polymers than the binding strength between individual water molecules at the interface.

1 Introduction

Adhesion of marine organisms to surfaces such as ships' hulls creates significant economic and environmental impacts on maritime shipping industries. Roughening of ships' hull surfaces by the growth of organisms, such as algae and barnacles, significantly increases drag and fuel consumption, while transoceanic voyages of fouling species are a leading vector for invasive species introduction in local ecosystems.[1, 2] Most commercially available marine antifouling coatings mitigate adhesion of organisms via controlled release of biocides, including organometals and copper oxides. The toxicity and bioaccumulation of these compounds, however, has resulted in increased regulation in recent years, prompting continued search for ecologically benign alternatives.[3, 4]

Zwitterionic polymers containing stoichiometrically balanced positive and negative charges are a promising alternative technology as stable, non-toxic coatings with remarkably low protein adsorption. Ion solvation at the polymer surface of these materials creates a strongly immobilized hydration layer at the interface, which acts as a physical and thermodynamic barrier to foulants.[5-8] These materials demonstrate extremely high performance in preventing biofilm formation for both membrane and biomedical applications, in addition to their more recent use in preventing adhesion of larger marine algae and hard foulers.[9-15]

While zwitterionic materials have been heavily studied for various fouling applications, the role of molecular design in zwitterion performance is poorly understood.[7, 8, 16-18] Existing studies

of the effects of ion size[17] and spacing distance[16] are restricted to variations of the most common betaine chemistries (carboxybetaine, sulfobetaine, and phosphorylcholine), leaving much of the design space unexplored. Among the explored chemistries, it remains unclear how these design parameters relate to surface properties that impact macroscale fouling resistance. Evaluation of marine antifouling coatings is heavily reliant on empirical assays, which lack insights into the molecular-scale mechanisms that impact performance. To address these challenges, this study uses a modular chemistry platform to systematically explore zwitterionic structure-property relationships across these microscopic to macroscopic length scales. The simplified surface architecture avoids the design complexities commonly employed in high performance antifouling coatings,[19-21] enabling improved understanding of specific design considerations rather than optimized overall performance. A combination of sum frequency generation (SFG) vibrational spectroscopy and marine assays correlates trends of surface hydration structure and marine fouling resistance to molecular structure, guiding the design of new polymeric zwitterion antifouling coatings.

One underexplored parameter in the design of zwitterionic antifouling coatings is the role of ion charge density on surface hydration and marine fouling. Both the hydration structure and backbone conformations of polymeric zwitterions are closely tied to the ionic character of the zwitterion functional groups. Self-associations between the cations and anions of adjacent polymer chains can cause aggregation behavior, while chain swelling is dependent on the charge density of the zwitterions and dissolved salt ions through the antipolyelectrolyte effect.[22-26] When exposed to salt solutions, polymeric zwitterions with low charge densities generally exhibit more swollen chain conformations than the more densely charged carboxybetaine and sulfobetaine chemistries.[17, 27, 28] Zwitterion antifouling performance is commonly associated with the level of

surface hydration, and hence, the increased chain swelling of diffuse polymeric zwitterions makes them candidate materials for marine antifouling applications. In this study, characterization of a series of polymeric zwitterion surfaces with increasingly delocalized charges show that more diffuse charges are more hydrated and exhibit reduced settlement and improved removal of the model algae foulant *Ulva linza*.

2 Experimental Methods

2.1 Materials

All chemicals were purchased from Sigma Aldrich and solvents from VWR and used as received unless specified otherwise. Trifluoromethanesulfonamide was purchased from TCI Chemicals. Hexamethylcyclotrisiloxane (D3) and 1,3,5-trivinyl-1,3,5-trimethylcyclotrisiloxane (V3) were purchased from Gelest, Inc. Anhydrous ethanol was purchased from Fisher Scientific. Benzene was stirred over n-butyl lithium and diphenylethylene, distilled and freeze-pump-thawed to degas. Styrene was dried over calcium hydride, distilled, and free-pump-thawed to degas. D3 was dissolved in benzene and stirred over calcium hydride for 24 hours at which point a living anionic styrene polymerization was added and allowed to stir until the orange color had completely disappeared. The benzene was subsequently distilled, and the D3 sublimed, and then the solution was freeze-pump-thawed to degas. This process was repeated one more time. Final solution concentration was determined using nuclear magnetic resonance spectroscopy (NMR). Tetrahydrofuran (THF) was stirred over calcium hydride and distilled into a flask containing sodium and benzophenone, and allowed to stir for several days, at which point it was distilled and freeze-pump-thawed to degas. V3 was stirred over calcium hydride, distilled, and freeze-pump-thawed to degas. Polystyrene-block-poly(ethylene-ran-butylene)-block-polystyrene (SEBS) and

polystyrene-block-poly(ethylene-ran-butylene)-block-polystyrene-graft-maleic anhydride (MA-SEBS) were generously provided by Kraton, Inc.

2.2 Polymer Synthesis

PS-P(DMS/VMS)-PS Backbone Synthesis

PS-P(DMS/VMS) backbones were prepared according to a previously reported method.[15, 29] In brief, in a glovebox *sec*-butyl lithium was added to a flask charged with benzene and a stir bar, followed by the dropwise addition of styrene, leading to the development of a deep orange color. The reaction progressed overnight before sampling, followed by the addition of a solution of D3 in benzene. After the complete disappearance of the orange color, indicative of the live styrene anion, THF was added and the reaction was allowed to continue for 2 hours. At this point, the addition of a solution of V3 in THF by syringe pump was begun and allowed to progress over 48 hours. After addition, the polymerization was reacted an additional 24 hours. The polymerization was then split, one half being end-capped with chlorotrimethylsilane for the formation of diblock, the other half coupled using a solution of dichlorodimethylsilane in THF. Coupling was done by adding 75% of coupling agent directly, followed by the addition of the remaining 25% of coupling agent by syringe pump over a 24-hour period. Polymers were precipitated directly into a 4/1 (v/v) mixture of methanol and deionized water and allowed to stir overnight. Polymers were collected by vacuum filtration and dried overnight in a vacuum oven at 55 ºC.

N-[3-(1H-imidazol-1-yl)propyl]-4-mercaptobutanamide (ImSH) Synthesis

Tertiary amine thiols were prepared according to previously reported methods.[30] The imidazole thiol (ImSH) was synthesized through ring opening of γ-thiobutyrolactone with 1-(3-

aminopropyl)imidazole. 40 mmoles of each γ-thiobutyrolactone and 1-(3-aminopropyl)imidazole were dissolved in 50 mL of HPLC grade acetonitrile in a 100 mL round-bottom flask. The flask was attached to a water-cooled condenser and quickly cycled thrice between nitrogen and vacuum on a Schlenk line to prevent disulfide formation. The flask was then left under a nitrogen blanket and refluxed with stirring at 95˚C overnight. After reaction, the acetonitrile was evaporated off and dried *in vacuo* at 60˚C overnight to yield a viscous, slightly yellow oil.

The alkylamine (AmSH) and pyridine (PyrSH) thiols were synthesized using the same procedure, replacing the 1-(3-aminopropyl)imidazole with either dimethylaminopropylamine or 3-(pyridine-4-yl)propan-1-amine, respectively.

AmSH: ^{1}H NMR (600 MHz, Chloroform-*d*) δ 7.13 (s, 1H), 3.20 (td, *J* = 6.5, 5.3 Hz, 2H), 2.46 (t, *J* = 7.0 Hz, 2H), 2.25 (t, *J* = 6.5 Hz, 2H), 2.18 (t, *J* = 7.3 Hz, 2H), 2.11 (s, 6H), 1.82 (q, *J* = 7.1 Hz, 2H), 1.53 (p, *J* = 6.5 Hz, 2H).

ImSH: ^{1}H NMR (600 MHz, Chloroform-*d*) δ 7.42 (d, *J* = 1.1 Hz, 1H), 7.01 (s, 1H), 6.91 (s, 1H), 6.38 (s, 1H), 3.96 (t, *J* = 6.9 Hz, 2H), 3.22 (q, *J* = 6.5 Hz, 2H), 2.54 (t, *J* = 6.9 Hz, 2H), 2.27 (t, *J* = 7.3 Hz, 2H), 2.00 – 1.91 (m, 2H), 1.89 (q, *J* = 7.1 Hz, 2H).

PyrSH: ^{1}H NMR (600 MHz, Chloroform-*d*) δ 8.48 – 8.42 (m, 2H), 7.11 – 7.06 (m, 2H), 5.76 (s, 1H), 3.26 (td, *J* = 7.1, 6.0 Hz, 2H), 2.65 – 2.58 (m, 2H), 2.55 (t, *J* = 6.9 Hz, 2H), 2.27 (t, *J* = 7.3 Hz, 2H), 1.91 (p, *J* = 7.0 Hz, 2H), 1.82 (p, *J* = 7.5 Hz, 2H).

Triethylammonium 3-Chloropropanesulfonyl-trifluorosulfonylimide (Cl-TFSI) Synthesis

The Cl-TFSI anion was prepared according to previously reported methods.[31] 10 g (1 equiv.) of trifluoromethanesulfonamide was dried in a 100 mL Schlenk flask, under vacuum, overnight. The following day, flask was transferred to a nitrogen blanket and the trifluoromethanesulfonamide was dissolved in 40 mL anhydrous acetonitrile and 28 mL (3 equiv.) triethylamine. In a second 100 mL Schlenk flask, 11.88 g (1 equiv.) of 3-chloropropanesulfonyl chloride was dissolved in 20 mL of anhydrous acetonitrile. The 3-chloropropanesulfonyl chloride

flask was then degassed with nitrogen bubbling for 20 minutes. The flask of 3-chloropropanesulfonyl chloride was chilled in an ice bath with stirring before transferring in the trifluoromethanesulfonamide solution dropwise with a syringe. The mixture was allowed to react overnight under a nitrogen blanket. The solution darkened and precipitated a yellow salt.

The following morning, the reaction mixture was filtered to remove the triethylammonium chloride salt. The solvent was removed, and the crude oil product was dissolved in 100 mL dichloromethane. This organic phase was washed with 100 mL water, 100 mL of 0.5 M HCl solution, and a final 100 mL water wash. The DCM was evaporated off, and then the purified product was dried *in vacuo* at 70° for 24 hours. The resulting product was a dark brown, viscous oil.

Thiol-ene Click of Amine Thiol to PS-P(DMS/VMS)-PS Backbone

1 equiv. of the PS-P(DMS/VMS)-PS backbone (measured by the pendant vinyl groups), 0.2 equiv. of 2,2-dimethoxy-2-phenylacetophenone, and 3 equiv. of the respective amine thiol (ImSH, AmSH, or PyrSH) were dissolved in inhibitor-free THF in a round-bottom flask. The flask was sealed and degassed under nitrogen bubbling for 20 minutes. The polymer was reacted by illumination under 365 nm UV exposure with stirring for 4 hours. Conversion was confirmed by the disappearance of the PVMS vinyl peaks in NMR. The clicked polymer was purified by precipitation in acetonitrile.

Formation of Zwitterionic Side Chains

The amine functionalized backbone was quaternized by mixing 1 equiv. thiol-ene clicked polymer with 2.5 equiv. of the chloro-TFSI anion in minimal anhydrous tetrahydrofuran. The reaction mixture was stirred at 60˚C for 5 days or until H-NMR confirmed full quaternization of

the amine functional groups, as indicated by downfield shifts in the nearby protons. The polymer was purified by precipitation in acetonitrile to remove the excess chloro-TFSI anion and triethylammonium chloride salt.

2.3 Sum Frequency Generation (SFG) Vibrational Spectroscopy

Three polymer samples were synthesized by the above-mentioned method. Each polymer sample was dissolved in anhydrous toluene (99.8%, Sigma-Aldrich, St. Louis, MO) with a concentration of 10 mg/mL. The prepared solution for each polymer was spin-coated onto right angle CaF_2 prisms (Altos Photonics, Bozeman, MT) at 3000 rpm for 30 seconds. After spin-coating, the CaF_2 prisms were heated at 120 ℃ under vacuum for 24 hours and cooled down to room temperature before SFG characterization.

SFG is a surface-sensitive technique involving second-order non-linear optical process. Detailed SFG theories and instrumentations have been published earlier and will not be repeated here.[6, 32, 33] Due to the selection rule, an SFG signal can only be produced where the inversion symmetry is broken, such as surface and interface.[6, 32, 33] With such a surface-sensitive property, SFG has been developed into a powerful tool to probe solid/air and solid/liquid interfaces, such as monitoring water behavior at the surface of zwitterionic polymers.[6] The SFG near-total-reflection sample geometry is used in this study as previously reported.[34] Briefly, a frequency-fixed visible beam at 532 nm and a frequency-tunable IR beam (1100 – 4300 cm^{-1}) were spatially and temporarily overlapped at the sample interface to generate a sum frequency signal beam ($\omega_{sum} = \omega_{vis} + \omega_{IR}$). In this study, SFG spectra were collected using the *ssp* (s-polarized SFG beam, s-polarized visible beam and p-polarized IR beam) and *ppp* polarization combinations.

To characterize the hydration of the polymer surfaces using SFG, each polymer surface was placed in contact with water, then SFG signal was collected from the polymer/water interface in the wavenumber region from 2750 to 3800 cm^{-1} after the SFG signal reached equilibrium. To test the antifouling property of the polymer surfaces with protein, a 1 mg/mL fibrinogen solution (dissolved in water) was used to replace the water originally in contact with the polymer surface. Then the fibrinogen solution was washed by fresh water three times to remove loosely adsorbed proteins. After equilibrium, the SFG signal was collected in the region from 1500 to 1800 cm^{-1} to probe the amide I signal of interfacial fibrinogen.

2.4 *Ulva linza* Fouling Assays

Before the assays were carried out, all the coatings were equilibrated for 72 hours in 0.22µm filtered artificial seawater (ASW) (Tropic Marin salts). Zoospores were obtained from mature plants of *U. linza* by the standard method.[35] After release from the fronds, the spores were collected and concentrated to produce a working suspension in ASW (1×10^6 spores ml^{-1}). Aliquots of 10 ml were added to quadriPERM dishes containing the coated slides. Spores were allowed to settle on the samples for 45 minutes in darkness at approximately 20˚C, after which the slides were washed to remove unsettled spores by moving backwards and forwards 10 times through a beaker of ASW. The attached spores were fixed in ASW containing 2.5% glutaraldehyde. The zoospore settlement densities were counted on 3 replicate slides of each sample using an image analysis system attached to a fluorescence microscope (Zeiss Axioskop 2) which detected the chlorophyll within individual cells. On each slide 30 fields of view (each 0.15 mm^2) were counted.

To culture *U. linza* on the samples, the initial settlement of spores was carried out as stated above. The settled spores were cultured into sporelings (young plants) on 6 replicate slides of each treatment using supplemented seawater medium.[36] The medium was refreshed every 2 days.

After 7 days of growth, sporeling biomass was measured in a Tecan fluorescence plate reader, which quantified the fluorescence from the chlorophyll contained in the plants. The measurement was given as relative fluorescence units (RFU). The RFU value for each sample was determined from 70 point fluorescence readings from the central area. The final biomass after 7 days was recorded as the average RFU from 6 replicate slides in conjunction with the standard error of the mean (SEM).

The strength of attachment of sporelings to the samples was determined by exposing the central region of each slide to an impact pressure of 132 kPa from an automated water jet. The amount of retained biomass was quantified using the fluorescence plate reader (as above) and used to calculate the percentage removal.

3 Results and Discussion

To elucidate the effects of zwitterion charge density on antifouling performance, we synthesized a series of side-chain functionalized siloxane polymer containing a range of cation charge densities (Figure 1). The alkylammonium cation acts as a control for the more commonly studied betaine chemistries while the imidazolium and pyridinium cations are increasingly more delocalized, yielding lower charge densities. All three cations are paired with the same diffusely charged sulfonamide anion with the same linker length between the anion and cation, yielding nearly equivalent dipole moments. A linker length of three methylene units was chosen to be

consistent with the bulk of existing literature which focuses on sulfobetaine chemistry. A fluorinated group attached to the sulfonamide drives surface segregation of the zwitterionic species.

The zwitterions are attached to a vinyl-functionalized siloxane polymer backbone via a two-step reaction. First, the amine cation precursor is thiol-ene clicked to the vinyl siloxane backbone. Then, the amine is quaternized with 3-chloropropanesulfonyl-trifluoromethanesulfonylimide (Cl-TFSI) to form the zwitterions (Scheme 1). The vinyl-functionalized siloxane polymer is capped on either end by polystyrene blocks to provide consistency with the existing surface-active block copolymer (SABC) approach for preparing marine assay samples, as detailed elsewhere.[37-39] The triblock copolymer architecture allows a thin layer (~20 μm) of the functional SABC material to be anchored into a much thicker (~500 μm) elastomeric base layer on the substrate, providing mechanical integrity and fouling release characteristics[40, 41] to the overall antifouling coating while minimizing the amount of functional zwitterionic polymer required. Zwitterionic samples are

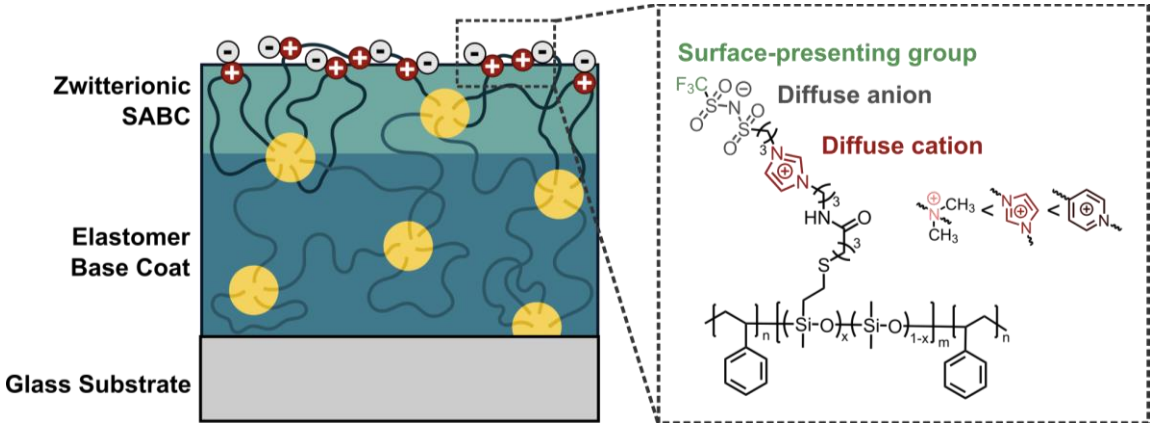

Figure 1. Marine fouling-resistant coatings are prepared using the surface-active block copolymer (SABC) approach where a thin layer of functional polymer is tethered to a thick elastomer base. This surface layer is functionalized with diffusely-charged zwitterionic groups and a fluorinated pendant end to drive surface segregation of the zwitterions. This work studies the effect of cation size by replacing the red cationic group with either ammonium, imidazolium or pyridinium.

labeled by abbreviated combinations of their cation and anion, as detailed in Table 1. Previous study of the SABC approach by ambient pressure X-ray photoelectron spectroscopy has shown that when hydrated, the polymer chains restructure, with the hydrophilic or fluorinated sidechains driven to the polymer/water interface.[42] Hence, the structure of the coatings is considered to be a dense film of hydrophobic polymer topped with a thin, hydrated layer of zwitterions.

Table 1. Cation/anion combinations of the polymeric zwitterion samples

Sample Name	Cation	Anion
AmTFSI	Alkylammonium	Trifluorosulfonylimide
ImTFSI	Imidazolium	Trifluorosulfonylimide
PyrTFSI	Pyridinium	Trifluorosulfonylimide

To understand the molecular-scale effects of cation charge density, sum frequency generation (SFG) vibrational spectroscopy probes the structure and dynamics of water molecules bound to the polymeric zwitterion surface. The SFG technique is sensitive only to media without inversion symmetry, enabling measurement of the hydration layer structure and molecular orientation perpendicular to the polymer/water interface.[43-45] Molecular details derived from SFG are then related to fouling performance through use of *Ulva linza* marine fouling assays.

We hypothesize that the more diffusely charged zwitterions enhance macrofouling resistance by creating a well-hydrated surface with more water molecules bound to the polymer coating. Here, we define the charge 'diffuseness' by the molecular volume over which the cation charge is delocalized. This can be quantified using group contributions methods, which yield the values presented in Table S2.[46-48] The number, binding strength, and orientational freedom of the surface-bound water are related to the size (or delocalization) of the charge and Coulombic electrostatic-dipole interactions between the cation and the water molecules (neglecting interactions of the diffuse anion for simplicity).[49] Due to their larger molecular volumes, the more diffuse charges can bind or interact with more water molecules at the ion surface, leading to a more hydrated

polymer/water interface. Since this interaction strength decays with distance from the charge center, larger, more diffuse ions will exhibit weaker zwitterion-solvent interactions with less restriction on the rotational and translational mobility of hydrated water molecules, which we thereby hypothesize minimizes disruption to the water hydrogen bond network. By mimicking both the structure and dynamics of bulk water, we expect these diffuse zwitterions to create a 'stealth' layer against macrofouling species.

Hydrated surface and fibrinogen assay SFG measurements support this hypothesis, showing that more diffuse cations (pyridinium and imidazolium) are well hydrated with overall more ordered, interfacial water molecules than the densely charged alkylammonium. SFG water O-H stretching signals usually have two broad peaks, centered at around 3200 cm^{-1} and 3400 cm^{-1}, assigned to the strongly hydrogen bonded and weakly hydrogen bonded water, respectively.[44, 50-52] Figure 2a shows that only very weak SFG water O-H stretching signals could be detected from the AmTFSI/water interface.

The SFG water signal shown here is not a direct measurement of the absolute quantity of bound water at the interface. Since SFG spectroscopy measures the net orientation vector of molecules in the system, water molecules oppositely oriented by the cation/anion pair will cancel out, with the

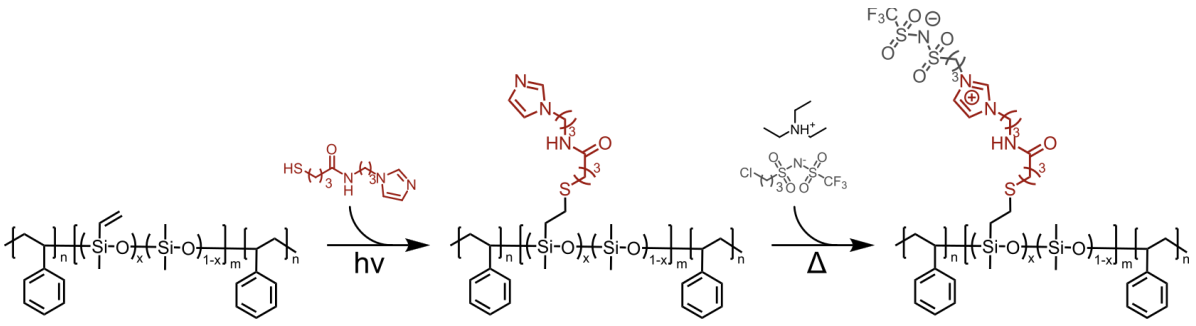

Scheme 1. The SABC is synthesized using a modular two-step approach, enabling facile customization of both the cation and anion. Here, the amine thiol is varied to contain alkylammonium, imidazolium, and pyridinium functionality.

resulting signal showing overall orientational imbalance in water structure. Since the three zwitterionic polymers have the same negative charge, the number and structure of the bound water molecules with the negative charges on the three polymers should be the same.

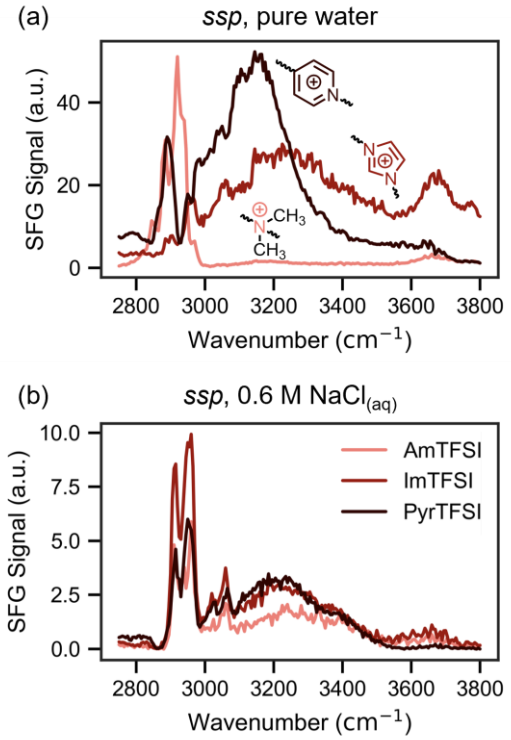

Figure 2. (a) Sum frequency generation spectroscopy (*ssp* polarization) of the different polymeric zwitterions shows that the larger, more diffuse cations bind more water molecules at the surface, as indicated by the intensity at 3200 cm^{-1}. (b) SFG spectra of the same materials in 0.6 M NaCl solution show the same hydration trend, but with weakened signal due to charge screening effects.

The measured SFG signals therefore suggest that delocalizing the cationic charge over a larger molecular volume in effect increases the coordination number of the cation, such that it can interact with additional water molecules that would otherwise be crowded out by excluded volume effects and screening of the electric field by the first hydration shell. As a result, more interfacial water molecules can be oriented by the cations compared to those by the anions, generating the SFG water signal. The siloxane midblock, the polystyrene end blocks, and the alkyl linkers between the charges are all hydrophobic and do not bind water molecules. The bound water at the interface should hence be primarily associated with the ion-dipole interactions to the zwitterions and directly correlated to the SFG signal.

Stronger SFG water signals detected from the more diffuse cations (PyrTFSI > ImTFSI > AmTFSI) displayed in Figure 2 are thus indicative of more ordered water molecules bound to the

cations by electrostatic-dipole interactions, supporting the above hypothesis. SFG spectra were measured in two different polarization combinations (*ssp* and *ppp*). These two polarization combinations probe different components of the samples' second-order nonlinear optical susceptibility (χ^2) tensors, and hence provide detail on different molecular orientations at the interface.[53] Both polarization combinations (Figures 2a and S9) show the same trend, suggesting that the surfaces have increased hydration rather than simply a preferred water orientation for the more delocalized cations.

Ionic strength has been previously shown to dramatically affect the performance of zwitterionic surfaces, either enhancing performance through the anti-polyelectrolyte effect or reducing performance by charge screening. Thus, to fully characterize the hydration state of these materials, *ssp* polarization SFG spectra were also taken in a 0.6 M solution of sodium chloride (the same ionic strength as seawater). As shown in Figure 2b, the surface hydration is greatly reduced on all three polymers, similar to what has been previously observed.[52] Despite this charge screening effect, the polymers still exhibit the same trend in hydration as the pure water SFG, supporting the conclusion that the diffuse charges are better hydrated and contribute to improved marine antifouling/fouling-release performance.

Fibrinogen adsorption assays on the zwitterionic surfaces suggest that the diffuse cations exhibit weaker binding of individual water molecules in their respective hydration shells, despite the overall increased surface hydration characterized by the bound water number at the interface. Fibrinogen possesses a net negative surface charge, and thus should selectively interact with the cationic group within the polymeric zwitterions. The quantity of adsorbed fibrinogen at the surface is characterized here by an SFG peak centered at ~1640 cm^{-1}, which corresponds to the amide C=O stretch.[34] A larger amide peak hence corresponds to more fibrinogen adsorbed to the interface. To

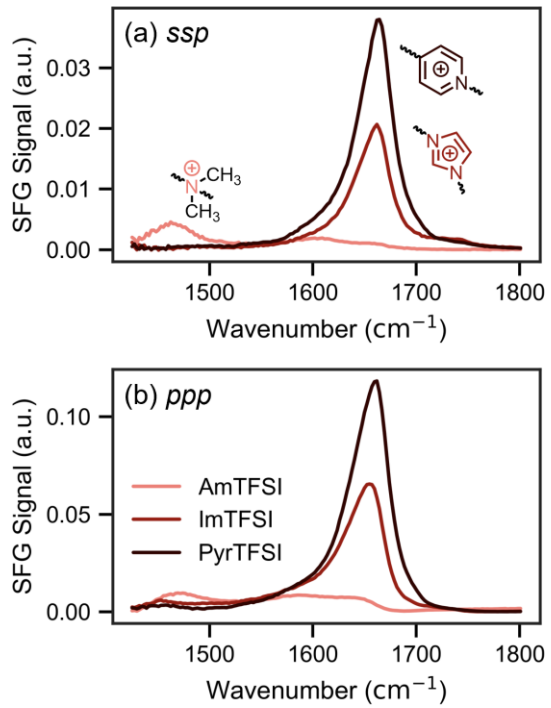

Figure 3. SFG fibrinogen protein assays in the (a) *ssp* and (b) *ppp* polarization combinations show stronger adsorption to the diffusely charged surfaces, suggesting that while more water molecules are adsorbed, they are only weakly bound to the zwitterionic surface, behaving more similarly to bulk water.

more reliably estimate the relative adsorption amount of fibrinogen, spectra were taken in both the *ssp* and *ppp* polarization combinations (Figure 3). The *ssp*/*ppp* amide peak ratios for each zwitterion type are similar, suggesting that the adsorbed fibrinogen macromolecules have similar orientations and the difference in signal is indicative of an increase in the quantity of adsorbed protein.

Interestingly, the more diffusely charged cations exhibit increased fibrinogen adsorption to the polymeric zwitterion surface after washing, despite the increased number of bound water molecules around the diffusely charged cations. Since protein adsorption requires displacement of these water molecules to reach the underlying polymer surface, increased adsorption suggests that the water molecules are more loosely bound to the diffuse cations. This matches expected results based on the relative Born solvation energies and interaction strengths of the cations.[49] As the charge is delocalized over a larger volume, the interaction strength between the charge and a given water molecule weakens. Both the trends in overall hydration and water binding strength are also in agreement with existing molecular dynamics simulations of betaine small molecules, which show that larger anions

coordinate a larger quantity of more weakly bound water molecules (as indicated by dipole orientations and residence time).[54]

Settlement and removal assays of *Ulva linza* correlate well with the extent of surface hydration observed by SFG, with the more diffusely charged, well hydrated zwitterions showing improved antifouling performance, especially in terms of foulant removal (Figure 4). To test antifouling performance of the zwitterionic coatings, the polymers were deposited and annealed into the multi-layered coatings shown in Figure 1. Substrates were then exposed to *U. linza* algal spores. Initial attachment densities of the spores were measured as well as their biomass after 7 days of growth. Adhesion strength to the surface was quantified by exposure to a calibrated water jet (to simulate the hydrodynamic forces experienced on a ship hull) with measurement of the change in attached biomass. A control sample of the unfunctionalized PS-P(VMS/DMS)-PS triblock copolymer was tested for comparison against the diffuse zwitterions.

Comparison between surface hydration by SFG and marine assays suggests interesting insights that link molecular scale surface properties and macroscale antifouling performance. In contrast to traditional theories of zwitterion antifouling mechanisms, here strong binding of water molecules at the polymer surface may not be the most important requirement for improved antifouling performance; rather, it is the increased overall hydration (or overall number of bound water molecules at the interface) that provides the advantage in marine applications. This behavior is hypothesized to be caused by the large difference in length scales of typical marine foulants and the protein/small molecule foulants used in biomedical and membrane antifouling studies, which results in different fouling and release mechanisms. Proteins foul on a molecular scale, through random collisions with the surface. In this case, displacement of only a few specific water molecules is required to reach the surface, with subsequent binding through either electrostatic

interactions or denaturation of the protein conformation. Prevention of fouling is thus achieved by maximizing the binding energy of those water molecules (as evidenced in Figure 3).

U. linza spores, however, are significantly larger than protein molecules and are also living organisms. Rather than relying on random collisions with the surface, these organisms undergo a brief "searching" phase during which they swim and explore the surface prior to settling. Studies of this behavior suggests that the spores are, to some extent, able to 'sense' and preferentially adhere to hydrophobic surfaces.[55-57] During this search process, the algal spore probes the surface hydration over a comparatively larger area, rather than judging the individual binding strength of the hydrated water molecules. In the larger length scale of the *U. linza* spore, zwitterion antifouling performance is thus improved by increased surface hydration with a larger quantity of bound

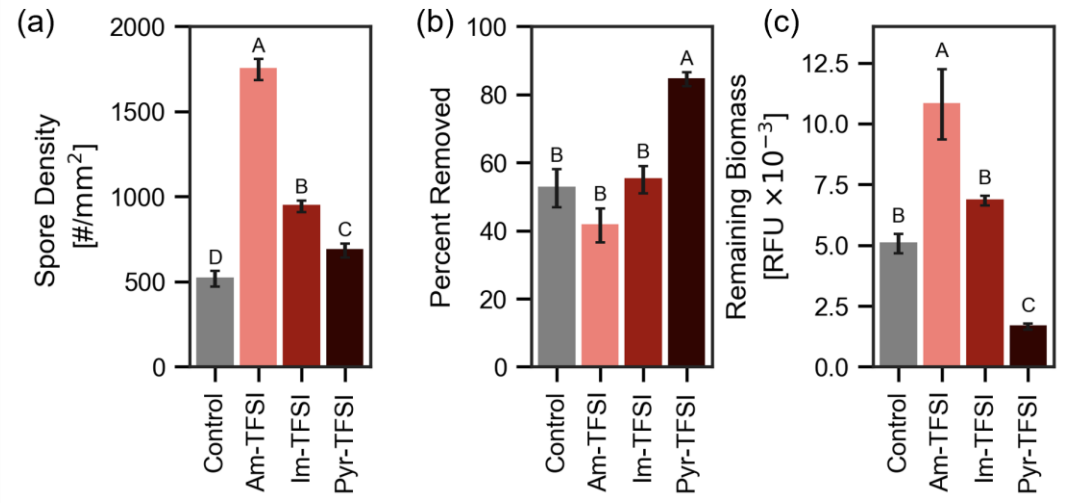

Figure 4. Marine fouling assays using *Ulva linza* show that the larger, more diffuse cations exhibit reduced algal settlement (a) and improved removal upon exposure to a water jet (b). Settled algae are also more weakly adhered to the diffusely-charged surfaces, leading to a minimal quantity of algae remaining on the surface after washing (c). Error bars indicate 95% confidence intervals for the settlement data and standard error of the means for removal and remaining biomass data. Letters above the error bars indicate statistical significance between samples, as calculated by Tukey's test.

interfacial water molecules, effectively hiding the polymer surface from the organism. This is reflected by the settlement assay results shown in Figure 4a, with the more diffusely charged and well-hydrated polymers showing reduced settlement of *U. linza* to the surface than the more densely charged polymers ($F_{5,534} = 636.7$; $p < 0.05$).

U. linza removal assays showed similar trends in performance, with the more diffusely charged samples demonstrating increased algal biomass removal ($F_{5,30} = 28$; $p < 0.05$). Since removal assays quantify the self-cleaning function of the coatings under the hydrodynamic shear forces experienced during a ship's voyage, this metric is most relevant to the fouling-release performance of the coatings. While the AmTFSI and ImTFSI samples are statistically similar to the nonfunctionalized triblock control (as indicated by Tukey's test), the PyrTFSI sample exhibits over 80% removal of accumulated sporeling biomass (Figure 4b).

Previous studies of *U. linza* have shown that while the spores typically prefer to settle on hydrophobic surfaces, the settled spores form stronger adhesive bonds to surfaces containing hydrogen-bond donors, which is thought to interact with the adhesive secreted by the spores.[58-60] Analogously, we conclude that the *U. linza* spores form stronger adhesive bonds to surfaces with dense cations (AmTFSI) compared to the diffuse cations (PyrTFSI). We hypothesize that this is a result of weakened electrostatic interactions experienced between the diffusely charged surfaces and the secreted glycoprotein adhesive network, as well as the increased levels of polymer surface hydration. This reduces the total number of surface contacts between the *U. linza* adhesive and the polymer coating as well as the strength of each contact (due to weakened Coulombic interactions), resulting in weaker bonding/adhesion of the algae to the coatings. Interestingly, this trend in *U. linza* removal also counters the results from the protein fouling assays, further demonstrating the differences in fouling mechanisms at these larger length scales.

Conclusions

This work utilizes a combination of surface-sensitive vibrational spectroscopy and marine fouling assays to analyze a new design motif of low charge density zwitterionic antifouling materials. SFG shows that larger, more delocalized cations create a well-hydrated surface, with more bound water molecules at the interface. The improved hydration of the delocalized cations reduces both the settlement frequency and adhesion strength of the alga *Ulva linza*, yielding improved fouling resistance and release performance over the more commonly studied alkylammonium cation. While the diffuse zwitterions show weaker resistance against protein adsorption and biofilm formation, a combined material approach containing diffuse zwitterions paired with other antifouling chemistries (e.g., amphiphilic,[61, 62] redox-active,[63] or protein-resistant trimethylamine N-oxide[8, 10] functionalities) may provide broader marine antifouling resistance.

Supporting Information

NMR spectra, images of coated slides from *Ulva linza* fouling assays, additional SFG data, additional discussion of cation size and marine assay performance.

Acknowledgements

This research was primarily supported by the Office of Naval Research awards N00014-16-1-2960, N00014-20-1-2248, N00014-20-1-2152, N00014-20-1-2234, N00014-23-1-2127, and N00014-23-1-2142. This work made use of the Cornell University NMR Facility, which is supported, in part, by the NSF through MRI award CHE-1531632. Polymer post-functionalization leveraged shared experimental facilities supported by the NSF MRSEC program under Award No. DMR 1720256. SDM acknowledges support from the National Science Foundation Graduate Research Fellowship (DGE 2139319).

References

1. He, M. R.; Gao, K.; Zhou, L. J.; Jiao, Z. W.; Wu, M. Y.; Cao, J. L.; You, X. D.; Cai, Z. Y.; Su, Y. L.; Jiang, Z. Y. Zwitterionic materials for antifouling membrane surface construction. *Acta Biomater* **2016**, *40*, 142-152. DOI: 10.1016/j.actbio.2016.03.038.
2. Ventura, C.; Guerin, A. J.; El-Zubir, O.; Ruiz-Sanchez, A. J.; Dixon, L. I.; Reynolds, K. J.; Dale, M. L.; Ferguson, J.; Houlton, A.; Horrocks, B. R.; et al. Marine antifouling performance of polymer coatings incorporating zwitterions. *Biofouling* **2017**, *33* (10), 892-903. DOI: 10.1080/08927014.2017.1383983.
3. Marechal, J. P.; Hellio, C. Challenges for the Development of New Non-Toxic Antifouling Solutions. *Int J Mol Sci* **2009**, *10* (11), 4623-4637. DOI: 10.3390/ijms10114623.
4. Jin, H. C.; Tian, L. M.; Bing, W.; Zhao, J.; Ren, L. Q. Bioinspired marine antifouling coatings: Status, prospects, and future. *Prog Mater Sci* **2022**, *124*. DOI: 10.1016/j.pmatsci.2021.100889.
5. Chen, S. F.; Li, L. Y.; Zhao, C.; Zheng, J. Surface hydration: Principles and applications toward low-fouling/nonfouling biomaterials. *Polymer* **2010**, *51* (23), 5283-5293. DOI: 10.1016/j.polymer.2010.08.022.
6. Chen, Z. Surface Hydration and Antifouling Activity of Zwitterionic Polymers. *Langmuir* **2022**, *38* (16), 4483-4489. DOI: 10.1021/acs.langmuir.2c00512.
7. Liu, Y. L.; Zhang, D.; Ren, B. P.; Gong, X.; Xu, L. J.; Feng, Z. Q.; Chang, Y.; He, Y.; Zheng, J. Molecular simulations and understanding of antifouling zwitterionic polymer brushes. *J Mater Chem B* **2020**, *8* (17), 3814-3828. DOI: 10.1039/d0tb00520g.
8. Huang, H.; Zhang, C. C.; Crisci, R.; Lu, T. Y.; Hung, H. C.; Sajib, M. S. J.; Sarker, P.; Ma, J. R.; Wei, T.; Jiang, S. Y.; et al. Strong Surface Hydration and Salt Resistant Mechanism of a New Nonfouling Zwitterionic Polymer Based on Protein Stabilizer TMAO. *J Am Chem Soc* **2021**, *143* (40), 16786-16795. DOI: 10.1021/jacs.1c08280.
9. Wei, H.; Insin, N.; Lee, J.; Han, H. S.; Cordero, J. M.; Liu, W. H.; Bawendi, M. G. Compact Zwitterion-Coated Iron Oxide Nanoparticles for Biological Applications. *Nano Lett* **2012**, *12* (1), 22-25. DOI: 10.1021/nl202721q.
10. Li, B. W.; Jain, P.; Ma, J. R.; Smith, J. K.; Yuan, Z. F.; Hung, H. C.; He, Y. W.; Lin, X. J.; Wu, K.; Pfaendtner, J.; et al. Trimethylamine N-oxide-derived zwitterionic polymers: A new class of ultralow fouling bioinspired materials. *Sci Adv* **2019**, *5* (6). DOI: 10.1126/sciadv.aaw9562.
11. Zhang, Z.; Finlay, J. A.; Wang, L. F.; Gao, Y.; Callow, J. A.; Callow, M. E.; Jiang, S. Y. Polysulfobetaine-Grafted Surfaces as Environmentally Benign Ultralow Fouling Marine Coatings. *Langmuir* **2009**, *25* (23), 13516-13521. DOI: 10.1021/la901957k.
12. Cheng, Q. L.; Asha, A. B.; Liu, Y.; Peng, Y. Y.; Diaz-Dussan, D.; Shi, Z. S.; Cui, Z. C.; Narain, R. Antifouling and Antibacterial Polymer-Coated Surfaces Based on the Combined Effect of Zwitterions and the Natural Borneol. *Acs Appl Mater Inter* **2021**, *13* (7), 9006-9014. DOI: 10.1021/acsami.0c22658.
13. van Andel, E.; de Bus, I.; Tijhaar, E. J.; Smulders, M. M. J.; Savelkoul, H. F. J.; Zuilhof, H. Highly Specific Binding on Antifouling Zwitterionic Polymer-Coated Microbeads as Measured by Flow Cytometry. *Acs Appl Mater Inter* **2017**, *9* (44), 38211-38221. DOI: 10.1021/acsami.7b09725.

14. Zhao, X. Z.; He, C. J. Efficient Preparation of Super Antifouling PVDF Ultrafiltration Membrane with One Step Fabricated Zwitterionic Surface. *Acs Appl Mater Inter* **2015**, *7* (32), 17947-17953. DOI: 10.1021/acsami.5b04648.
15. Higaki, Y.; Nishida, J.; Takenaka, A.; Yoshimatsu, R.; Kobayashi, M.; Takahara, A. Versatile inhibition of marine organism settlement by zwitterionic polymer brushes. *Polym J* **2015**, *47* (12), 811-818. DOI: 10.1038/pj.2015.77.
16. Shao, Q.; Jiang, S. Y. Effect of Carbon Spacer Length on Zwitterionic Carboxybetaines. *J Phys Chem B* **2013**, *117* (5), 1357-1366. DOI: 10.1021/jp3094534.
17. Shao, Q.; Mi, L.; Han, X.; Bai, T.; Liu, S. J.; Li, Y. T.; Jiang, S. Y. Differences in Cationic and Anionic Charge Densities Dictate Zwitterionic Associations and Stimuli Responses. *J Phys Chem B* **2014**, *118* (24), 6956-6962. DOI: 10.1021/jp503473u.
18. Shao, Q.; Jiang, S. Y. Molecular Understanding and Design of Zwitterionic Materials. *Adv Mater* **2015**, *27* (1), 15-26. DOI: 10.1002/adma.201404059.
19. Zhang, D.; Ren, B. P.; Zhang, Y. X.; Liu, Y. L.; Chen, H.; Xiao, S. W.; Chang, Y.; Yang, J. T.; Zheng, J. Micro- and macroscopically structured zwitterionic polymers with ultralow fouling property. *J Colloid Interf Sci* **2020**, *578*, 242-253. DOI: 10.1016/j.jcis.2020.05.122.
20. Dai, G. X.; Xie, Q. Y.; Ai, X. Q.; Ma, C. F.; Zhang, G. Z. Self-Generating and Self-Renewing Zwitterionic Polymer Surfaces for Marine Anti-Biofouling. *Acs Appl Mater Inter* **2019**, *11* (44), 41750-41757. DOI: 10.1021/acsami.9b16775.
21. Li, X. H.; Tang, C. J.; Liu, D.; Yuan, Z. F.; Hung, H. C.; Luozhong, S.; Gu, W. C.; Wu, K.; Jiang, S. Y. High-Strength and Nonfouling Zwitterionic Triple-Network Hydrogel in Saline Environments. *Adv Mater* **2021**, *33* (39), 2102479. DOI: 10.1002/adma.202102479.
22. Erfani, A.; Seaberg, J.; Aichele, C. P.; Ramsey, J. D. Interactions between Biomolecules and Zwitterionic Moieties: A Review. *Biomacromolecules* **2020**, *21* (7), 2557-2573. DOI: 10.1021/acs.biomac.0c00497.
23. Petroff, M. G.; Garcia, E. A.; Herrera-Alonso, M.; Bevan, M. A. Ionic Strength-Dependent Interactions and Dimensions of Adsorbed Zwitterionic Copolymers. *Langmuir* **2019**, *35* (14), 4976-4985. DOI: 10.1021/acs.langmuir.9b00218.
24. Shao, Q.; He, Y.; Jiang, S. Y. Molecular Dynamics Simulation Study of Ion Interactions with Zwitterions. *J Phys Chem B* **2011**, *115* (25), 8358-8363. DOI: 10.1021/jp204046f.
25. Delgado, J. D.; Schlenoff, J. B. Static and Dynamic Solution Behavior of a Polyzwitterion Using a Hofmeister Salt Series. *Macromolecules* **2017**, *50* (11), 4454-4464. DOI: 10.1021/acs.macromol.7b00525.
26. He, Q. M.; Qiao, Y. J.; Jimenez, C. M.; Hackler, R.; Martinson, A. B. F.; Chen, W.; Tirrell, M. V. Ion Specificity Influences on the Structure of Zwitterionic Brushes. *Macromolecules* **2023**, *56* (5), 1945-1953. DOI: 10.1021/acs.macromol.2c02029.
27. Xiao, S. W.; Zhang, Y. X.; Shen, M. X.; Chen, F.; Fan, P.; Zhong, M. Q.; Ren, B. P.; Yang, J. T.; Zheng, J. Structural Dependence of Salt-Responsive Polyzwitterionic Brushes with an Anti-Polyelectrolyte Effect. *Langmuir* **2018**, *34* (1), 97-105. DOI: 10.1021/acs.langmuir.7b03667.
28. Chen, H.; Yang, J. T.; Xiao, S. W.; Hu, R. D.; Bhaway, S. M.; Vogt, B. D.; Zhang, M. Z.; Chen, Q.; Ma, J.; Chang, Y.; et al. Salt-responsive polyzwitterionic materials for surface regeneration between switchable fouling and antifouling properties. *Acta Biomater* **2016**, *40*, 62-69. DOI: 10.1016/j.actbio.2016.03.009.
29. Leonardi, A. K.; Medhi, R.; Zhang, A. R.; Duzen, N.; Finlay, J. A.; Clarke, J. L.; Clare, A. S.; Ober, C. K. Investigation of N-Substituted Morpholine Structures in an Amphiphilic PDMS-

Based Antifouling and Fouling-Release Coating. *Biomacromolecules* **2022**, *23* (6), 2697-2712. DOI: 10.1021/acs.biomac.1c01474.
30. Sanoja, G. E.; Schauser, N. S.; Bartels, J. M.; Evans, C. M.; Helgeson, M. E.; Seshadri, R.; Segalman, R. A. Ion Transport in Dynamic Polymer Networks Based on Metal-Ligand Coordination: Effect of Cross-Linker Concentration. *Macromolecules* **2018**, *51* (5), 2017-2026. DOI: 10.1021/acs.macromol.7b02141.
31. Matsumoto, K.; Endo, T. Synthesis of Networked Polymers by Copolymerization of Monoepoxy-Substituted Lithium Sulfonylimide and Diepoxy-Substituted Poly(ethylene glycol), and Their Properties. *J Polym Sci Pol Chem* **2011**, *49* (8), 1874-1880. DOI: 10.1002/pola.24614.
32. Lu, X. L.; Zhang, C.; Ulrich, N.; Xiao, M. Y.; Ma, Y. H.; Chen, Z. Studying Polymer Surfaces and Interfaces with Sum Frequency Generation Vibrational Spectroscopy. *Anal Chem* **2017**, *89* (1), 466-489. DOI: 10.1021/acs.analchem.6b04320.
33. Guo, W.; Lu, T. Y.; Gandhi, Z.; Chen, Z. Probing Orientations and Conformations of Peptides and Proteins at Buried Interfaces. *J Phys Chem Lett* **2021**, *12* (41), 10144-10155. DOI: 10.1021/acs.jpclett.1c02956.
34. Wang, J.; Even, M. A.; Chen, X. Y.; Schmaier, A. H.; Waite, J. H.; Chen, Z. Detection of amide I signals of interfacial proteins in situ using SFG. *J Am Chem Soc* **2003**, *125* (33), 9914-9915. DOI: 10.1021/ja036373s.
35. Finlay, J.; Callow, M. E.; Schultz, M. P.; Swain, G. W.; Callow, J. A. Adhesion Strength of Settled Spores of the Green Alga *Enteromorpha*. *Biofouling* **2002**, *18* (4), 251-256. DOI: 10.1080/08927010290029010.
36. Starr, R. C.; Zeikus, J. A. Utex - the Culture Collection of Algae at the University-of-Texas at Austin 1993 List of Cultures. *J Phycol* **1993**, *29* (2), 1-106. DOI: 10.1111/j.0022-3646.1993.00001.x.
37. Patterson, A. L.; Wenning, B.; Rizis, G.; Calabrese, D. R.; Finlay, J. A.; Franco, S. C.; Zuckermann, R. N.; Clare, A. S.; Kramer, E. J.; Ober, C. K.; et al. Role of Backbone Chemistry and Monomer Sequence in Amphiphilic Oligopeptide- and Oligopeptoid-Functionalized PDMS- and PEO-Based Block Copolymers for Marine Antifouling and Fouling Release Coatings. *Macromolecules* **2017**, *50* (7), 2656-2667. DOI: 10.1021/acs.macromol.6b02505.
38. Weinman, C. J.; Finlay, J. A.; Park, D.; Paik, M. Y.; Krishnan, S.; Sundaram, H. S.; Dimitriou, M.; Sohn, K. E.; Callow, M. E.; Callow, J. A.; et al. ABC Triblock Surface Active Block Copolymer with Grafted Ethoxylated Fluoroalkyl Amphiphilic Side Chains for Marine Antifouling/Fouling-Release Applications. *Langmuir* **2009**, *25* (20), 12266-12274. DOI: 10.1021/la901654q.
39. Krishnan, S.; Ayothi, R.; Hexemer, A.; Finlay, J. A.; Sohn, K. E.; Perry, R.; Ober, C. K.; Kramer, E. J.; Callow, M. E.; Callow, J. A.; et al. Anti-biofouling properties of comblike block copolymers with amphiphilic side chains. *Langmuir* **2006**, *22* (11), 5075-5086. DOI: 10.1021/la052978l.
40. Gray, N. L.; Banta, W. C.; Loeb, G. I. Aquatic biofouling larvae respond to differences in the mechanical properties of the surface on which they settle. *Biofouling* **2002**, *18* (4), 269-273. DOI: 10.1080/0892701021000034373.
41. Chaudhury, M. K.; Finlay, J. A.; Chung, J. Y.; Callow, M. E.; Callow, J. A. The influence of elastic modulus and thickness on the release of the soft-fouling green alga (syn. Enteromorpha linza) from poly(dimethylsiloxane) (PDMS) model networks. *Biofouling* **2005**, *21* (1), 41-48. DOI: 10.1080/08927010500044377.

42. Barry, M. E.; Gokturk, P. A.; DeStefano, A. J.; Leonardi, A. K.; Ober, C. K.; Crumlin, E. J.; Segalman, R. A. Effects of Amphiphilic Polypeptoid Side Chains on Polymer Surface Chemistry and Hydrophilicity. *Acs Appl Mater Inter* **2022**, *14* (5), 7340-7349. DOI: 10.1021/acsami.1c22683.
43. Del Grosso, C. A.; Leng, C.; Zhang, K. X.; Hung, H. C.; Jiang, S. Y.; Chen, Z.; Wilker, J. J. Surface hydration for antifouling and bio-adhesion. *Chem Sci* **2020**, *11* (38), 10367-10377. DOI: 10.1039/d0sc03690k.
44. Leng, C.; Sun, S. W.; Zhang, K. X.; Jiang, S. Y.; Chen, Z. Molecular level studies on interfacial hydration of zwitterionic and other antifouling polymers in situ. *Acta Biomater* **2016**, *40*, 6-15. DOI: 10.1016/j.actbio.2016.02.030.
45. Zhang, C.; Myers, J. N.; Chen, Z. Elucidation of molecular structures at buried polymer interfaces and biological interfaces using sum frequency generation vibrational spectroscopy. *Soft Matter* **2013**, *9* (19), 4738-4761. DOI: 10.1039/c3sm27710k.
46. Ye, C. F.; Shreeve, J. M. Rapid and accurate estimation of densities of room-temperature ionic liquids and salts. *J Phys Chem A* **2007**, *111* (8), 1456-1461. DOI: 10.1021/jp066202k.
47. Gianni, P.; Lepori, L. Group contributions to the partial molar volume of ionic organic solutes in aqueous solution. *J Solution Chem* **1996**, *25* (1), 1-42. DOI: 10.1007/Bf00972756.
48. Lepori, L.; Gianni, P. Partial molar volumes of ionic and nonionic organic solutes in water: A simple additivity scheme based on the intrinsic volume approach. *J Solution Chem* **2000**, *29* (5), 405-447. DOI: 10.1023/A:1005150616038.
49. Israelachvili, J. N. *Intermolecular and surface forces*; Academic Press, 2011.
50. Leng, C.; Hung, H. C.; Sun, S. W.; Wang, D. Y.; Li, Y. T.; Jiang, S. Y.; Chen, Z. Probing the Surface Hydration of Nonfouling Zwitterionic and PEG Materials in Contact with Proteins. *Acs Appl Mater Inter* **2015**, *7* (30), 16881-16888. DOI: 10.1021/acsami.5b05627.
51. Leng, C.; Hung, H. C.; Sieggreen, O. A.; Li, Y. T.; Jiang, S. Y.; Chen, Z. Probing the Surface Hydration of Nonfouling Zwitterionic and Poly(ethylene glycol) Materials with Isotopic Dilution Spectroscopy. *J Phys Chem C* **2015**, *119* (16), 8775-8780. DOI: 10.1021/acs.jpcc.5b01649.
52. Leng, C.; Han, X. F.; Shao, Q.; Zhu, Y. H.; Li, Y. T.; Jiang, S. Y.; Chen, Z. In Situ Probing of the Surface Hydration of Zwitterionic Polymer Brushes: Structural and Environmental Effects. *J Phys Chem C* **2014**, *118* (29), 15840-15845. DOI: 10.1021/jp504293r.
53. Chen, Z. Investigating buried polymer interfaces using sum frequency generation vibrational spectroscopy. *Prog Polym Sci* **2010**, *35* (11), 1376-1402. DOI: 10.1016/j.progpolymsci.2010.07.003.
54. Shao, Q.; He, Y.; White, A. D.; Jiang, S. Y. Difference in Hydration between Carboxybetaine and Sulfobetaine. *J Phys Chem B* **2010**, *114* (49), 16625-16631. DOI: 10.1021/jp107272n.
55. Finlay, J. A.; Krishnan, S.; Callow, M. E.; Callow, J. A.; Dong, R.; Asgill, N.; Wong, K.; Kramer, E. J.; Ober, C. K. Settlement of Ulva zoospores on patterned fluorinated and PEGylated monolayer surfaces. *Langmuir* **2008**, *24* (2), 503-510. DOI: 10.1021/la702275g.
56. Callow, M. E.; Callow, J. A.; Ista, L. K.; Coleman, S. E.; Nolasco, A. C.; Lopez, G. P. Use of self-assembled monolayers of different wettabilities to study surface selection and primary adhesion processes of green algal (Enteromorpha) zoospores. *Appl Environ Microb* **2000**, *66* (8), 3249-3254. DOI: 10.1128/Aem.66.8.3249-3254.2000.
57. Heydt, M.; Pettitt, M. E.; Cao, X.; Callow, M. E.; Callow, J. A.; Grunze, M.; Rosenhahn, A. Settlement Behavior of Zoospores of Ulva linza During Surface Selection Studied by Digital Holographic Microscopy. *Biointerphases* **2012**, *7* (1-4). DOI: 10.1007/s13758-012-0033-y.

58. Callow, J. A.; Callow, M. E.; Ista, L. K.; Lopez, G.; Chaudhury, M. K. The influence of surface energy on the wetting behaviour of the spore adhesive of the marine alga Ulva linza (synonym Enteromorpha linza). *J Roy Soc Interface* **2005**, *2* (4), 319-325. DOI: 10.1098/rsif.2005.0041.
59. Finlay, J. A.; Callow, M. E.; Ista, L. K.; Lopez, G. P.; Callow, J. A. The influence of surface wettability on the adhesion strength of settled spores of the green alga Enteromorpha and the diatom Amphora. *Integr Comp Biol* **2002**, *42* (6), 1116-1122. DOI: 10.1093/icb/42.6.1116.
60. Barry, M. E.; Davidson, E. C.; Zhang, C. C.; Patterson, A. L.; Yu, B. H.; Leonardi, A. K.; Duzen, N.; Malaviya, K.; Clarke, J. L.; Finlay, J. A.; et al. The Role of Hydrogen Bonding in Peptoid-Based Marine Antifouling Coatings. *Macromolecules* **2019**, *52* (3), 1287-1295. DOI: 10.1021/acs.macromol.8b02390.
61. van Zoelen, W.; Buss, H. G.; Ellebracht, N. C.; Lynd, N. A.; Fischer, D. A.; Finlay, J.; Hill, S.; Callow, M. E.; Callow, J. A.; Kramer, E. J.; et al. Sequence of Hydrophobic and Hydrophilic Residues in Amphiphilic Polymer Coatings Affects Surface Structure and Marine Antifouling/Fouling Release Properties. *Acs Macro Lett* **2014**, *3* (4), 364-368. DOI: 10.1021/mz500090n.
62. Zhou, Z. L.; Calabrese, D. R.; Taylor, W.; Finlay, J. A.; Callow, M. E.; Callow, J. A.; Fischer, D.; Kramer, E. J.; Ober, C. K. Amphiphilic triblock copolymers with PEGylated hydrocarbon structures as environmentally friendly marine antifouling and fouling-release coatings. *Biofouling* **2014**, *30* (5), 589-604. DOI: 10.1080/08927014.2014.897335.
63. Leonardi, A.; Zhang, A. C.; Duzen, N.; Aldred, N.; Finlay, J. A.; Clarke, J. L.; Clare, A. S.; Segalman, R. A.; Ober, C. K. Amphiphilic Nitroxide-Bearing Siloxane-Based Block Copolymer Coatings for Enhanced Marine Fouling Release. *Acs Appl Mater Inter* **2021**, *13* (24), 28790-28801. DOI: 10.1021/acsami.1c05266.

TOC Graphic

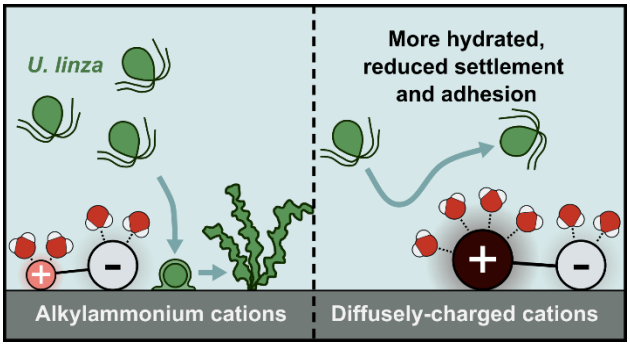
U. linza
More hydrated,
reduced settlement
and adhesion
Alkylammonium cations
Diffusely-charged cations